

Article

Design and Validation of an Instrument for Noninvasive Measurement of Connecting Rod Deformation in Spark Ignition Engines for Hybrid Vehicles

Vincenzo La Battaglia ¹, Livia Del Pinto ¹, Stefano Marini ¹, Alessandro Giorgetti ^{1,*} and Gabriele Arcidiacono ²

¹ Department of Industrial, Electronic and Mechanical Engineering, Roma Tre University, 00146 Rome, Italy; vincenzo.labattaglia@uniroma3.it (V.L.B.); liv.delpinto@stud.uniroma3.it (L.D.P.); stefano.marini@uniroma3.it (S.M.)

² Department of Engineering Science, Guglielmo Marconi University, 00193 Rome, Italy; g.arcidiacono@unimarconi.it

* Correspondence: alessandro.giorgetti@uniroma3.it

Abstract

This work presents the development of a measuring instrument capable of assessing the possible presence of critical permanent deformations on the connecting rod in hybrid cars equipped with gasoline-powered internal combustion engines. The permanent deformation can be due to incorrect fueling and cause a progressive engine failure through the breaking of one or more connecting rods. The measuring tool developed is a non-invasive, low-cost system and permits the detection of the incipient damage without dismantling the engine, thus assuring a time-saving approach. The instrument is composed of a mechanical system and an electronic interface that permits easy use during measuring operations and the possibility to store the data collected. An experimental campaign was implemented to validate the measurement system's capability to detect this type of damage and to determine a threshold beyond which it is necessary to proceed with the replacement of connecting rods. The results show the optimal ability to differentiate between usual technological variability of the piston stroke and the range that can be connected to the anomaly studied. The system is also able to permit the measurement of a whole engine in less than 20 min.

Keywords: measurement system; hybrid vehicle; connecting rod deformation; non-invasive measurement technique; spark ignition engines



Academic Editor: Ruxandra Botez

Received: 19 December 2025

Revised: 28 January 2026

Accepted: 3 February 2026

Published: 5 February 2026

Copyright: © 2026 by the authors.

Licensee MDPI, Basel, Switzerland.

This article is an open access article distributed under the terms and

conditions of the [Creative Commons Attribution \(CC BY\) license](https://creativecommons.org/licenses/by/4.0/).

1. Introduction

The ever-increasing diffusion of electric technology in modern vehicles has led to highly diversified hybrid vehicle architectures to improve the efficiency of the power generation [1–4]. The introduction of electric machines into the powertrain entails both new design criteria [5] for some vehicle components [6–8] that must consider the fact that the internal combustion engine may not always be running (see, for example, the vacuum pump for the depression used in the brake booster, the operation of the air conditioning compressor, etc.). Another aspect is that the presence of the electric machine allows for the use of smaller or less powerful engines but with higher efficiency. A possible configuration is based on the use of a variable compression ratio (VCR) system that permits them to

operate at a higher compression ratio under lower loads, which would reduce pumping losses and fuel consumption [9].

Furthermore, hybrid architecture can create issues related to the vehicle's actual usage, potentially leading to anomalies that are difficult to prevent during the design phase [10–14]. For example, the literature analyzes the effects of refueling internal combustion engines with fuel adulterated with water, chlorine, and other substances on their various components [15].

The after-sales service of hybrid cars equipped with gasoline-powered internal combustion engines has also encountered another type of issue due to the incorrect fueling that has led to the return of vehicles for service. One of the observed cases involves repairs following the incorrect filling of diesel fuel instead of gasoline during refueling. Repairs include cleaning the tank and lines, checking the injectors, and checking the fuel pumps. In some cases, after the vehicle has been repaired and the owner has driven a range of kilometers (usually from a few hundred to a few thousand kilometers), the engine fails. The failure happens when one or more connecting rods break, causing mechanical interference between the components.

This occurs because in some types of hybrid vehicles, the internal combustion engine is driven by the electric motor due to the presence of a planetary gearbox in the transmission [16–18]. This architecture may lead to two scenarios if the fuel mixture is incorrect, depending on the particular gasoline-to-diesel ratio: if the gasoline quantity is sufficient to start combustion, it may be less violent than expected but occur irregularly due to the simultaneous presence of diesel fuel, which ignites through spontaneous combustion under appropriate pressure and temperature conditions, thereby overlapping the effects of both combustion processes. If the quantity of diesel fuel predominates, ignition fails to occur, leading to an accumulation of unburned mixture in the combustion chamber. The two forms of anomalies may put a force on the piston crowns that exceeds acceptable limits, potentially causing structural damage to the connecting rods. This effect is even more pronounced in Miller cycle engines, usually adopted in hybrid vehicles, which have lower compression ratios than Otto cycle engines [19,20]; these engines are designed with structural components that can handle lower peak loads, thereby achieving better efficiency and energy savings through a lightweight approach [21–24].

In conventional vehicles, the driver instantly perceives the anomalous operation of the engine, including irregular torque at the wheels. Furthermore, if the ignition fails, the vehicle cannot be used because the engine will not start. Instead in hybrid vehicles, the presence of the electric motor that drives the combustion engine tends to regulate traction, masking this malfunction. Operation of the hybrid vehicle under incorrect fueling, sometimes even prolonged for the reasons described, could therefore cause plastic deformations to the connecting rods to such an extent that, on the one hand, they do not produce evident signs of damage, like the classic knocking sound, and therefore may not be detected during vehicle repairs. On the other hand, they could not generate permanent deformation that causes the crankshaft to operate abnormally and cause self-degenerative damage that, over time, can lead to the collapse of the engine structure. Consequently, the subsequent breakage is not attributable to a manufacturing defect but to incorrect use and so the warranty cannot be applied.

To identify the origin of the damage, it is possible to examine the integrity of the connecting rods during vehicle repairs following incorrect refueling, but the procedure currently used is extremely time-consuming and complex. It involves the disassembly of the connecting rods and checking their geometry (e.g., linearity of the connecting rod axis, presence of twists, etc.), which can be obtained only after dismantling the engine block. The whole procedure duration is approximately 20 h and consists of more than 50 operations,

and the procedure cost can be evaluated in the range 2000–4000 Euros depending on the labor cost. The cost of this procedure is borne by the car owner.

Therefore, the need arises to be able to assess the integrity of the connecting rods more easily without having to disassemble the engine.

A first option would be to evaluate the compression values in the cylinders using the equipment typically used for compression tests, which is already available in repair workshops. However, this procedure is not capable of reliably detecting slight deformations of the connecting rod, which, while not leading to immediate engine failure, do threaten its short-term service life (the reference range described above). This occurs because such deformations generate effects that fall within the normal combustion pressure tolerance set by OEMs, which is approximately more than 1 bar [25,26]. This tolerance value results in an uncertainty in the piston stroke estimated at approximately 1 mm, and consequently, it can be assumed that even significant deformations of the connecting rod attributable to the cases described above could fall within the normal pressure tolerances measured with this test. Furthermore, the compression test is indicative of the effects of the decrease in pressure reached in the various cylinders due to various causes (piston ring wear, imperfect couplings, imperfect valve sealing, etc.), which would lead to false positives due to other causes. The compression test is therefore not suitable for obtaining useful information in the case in question.

This paper aims to create a specific measuring device that can assess the existence of critical permanent deformations on the connecting rod in a non-invasive way, and which is able to detect such defects with a reduced number of operations and reduced times without disassembling the engine.

The structure of the paper is organized as follows. Section 2 introduces the collection of design specifications and constraints, as well as the design concept. Then the instrument's mechanical parts, user interface, and measurement procedure are shown. The experimental validation of the approach is presented in Section 3, and Section 4 summarizes the conclusions of the paper.

2. Materials and Methods

This section offers a concise and precise description of the system, beginning with the concept and architecture definition, followed by the description of the components and the hardware and software interface, and concluding with the definition of the measurement procedure.

2.1. Concept of the Instrument

To develop a tool that is suitable for the previously identified task, the various characteristics and requirements that must characterize the project are collected and analyzed.

2.1.1. Definition of System Specifications and Dimensional Constraints

The instrument must be capable of measuring the actual stroke of the pistons inside the cylinders. The measurement must be performed without having to disconnect the engine from the vehicle and disassemble it. Furthermore, it must be suitable for use in mechanical workshops, even by non-highly specialized operators, ensuring robustness and ease of use. It must be suitable for measuring various types of hybrid vehicles, even with different engine types.

The solution identified for performing this type of measurement is to evaluate the piston's movement within the cylinder using the spark plug opening in the cylinder head. This solution would eliminate any disassembly other than removing the ignition coil assembly and spark plug, an operation that takes just a few minutes.

In order to assess the dimensional constraints on the instrument's overall size, measurements were performed on a sample of vehicles equipped with hybrid architecture. This was carried out to examine the engine's layout within the engine compartment and, in more detail, assess whether the instrument's mounting opening, represented by the spark plug tubes, or their projection, interfered with other vehicle components. Observations indicated that the engine installed on some models was tilted a few degrees toward the passenger compartment; this implies that the spark plug tubes were also tilted and pointed toward the rainwater tank beneath the windshield wipers (Figure 1). From a dimensional standpoint, the maximum size available in this direction in vehicles with more stringent constraints was found to be about 125 mm. The instrument must therefore have an overall length such that the part protruding from the tubes is less than this value to avoid having to dismantle the windshield wipers and the rainwater connection tray to take the measurement. This dimensional constraint is not trivial to respect, as the depth of the tubes is measured at 150 mm, and it is also necessary to plan for the insertion phase of the instrument.

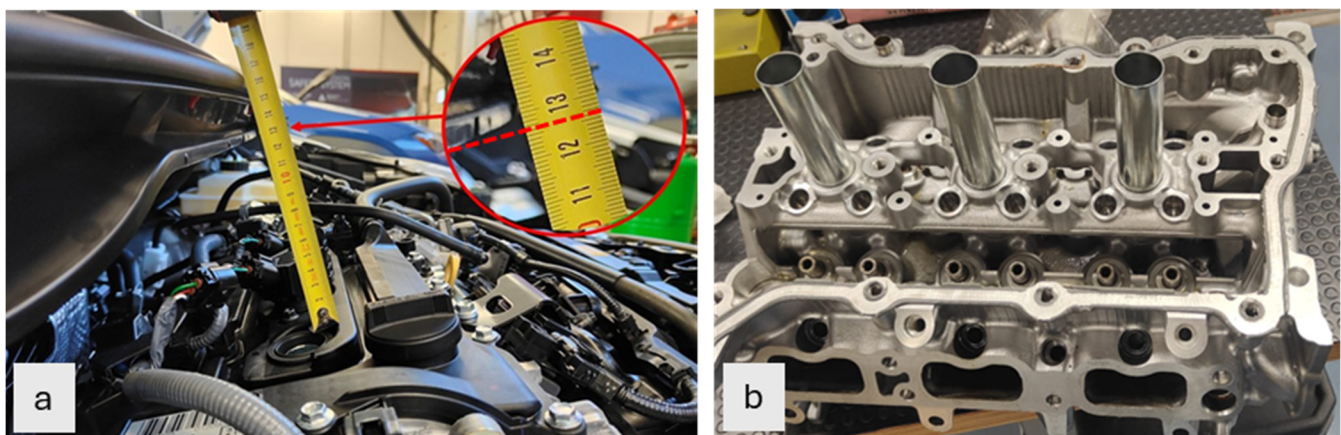


Figure 1. (a) Maximum permitted size of the instrument (red dashed line); (b) cylinder head with the three spark plug tubes.

Regarding the radial dimension of the instrument, the diameter of the tubes measured was 21.7 mm, thus identifying this value as the maximum dimension for the diameter of the instrument. Another dimensional constraint is represented by the spark plug thread, which was a 12 mm fine-pitch metric thread ($M12 \times 1.25$) with a threaded hole length in the cylinder head of 25 mm.

In order to perform an absolute measurement, it is necessary to identify a unique reference point for all cylinders and engines. The design choice identified the spark plug reference surface at the top of the cylinder head as the surface to be used for this task. This assumption implies that the dimensional error relating to the position of this surface with respect to the position of the top dead center to be measured is acceptable for detecting the connecting rod deformation ranges typical of the anomaly studied.

2.1.2. Definition of the System Architecture

The project specifications require evaluating the piston stroke in the cylinder; therefore, various measuring instruments capable of measuring linear displacement were considered. The presence of the tubes and the space limitations described above prevent the direct use of commercial measuring instruments (such as calipers, comparators, LVDTs, and laser rangefinders).

A system is therefore being studied to be able to precisely transfer the piston movement above the tubes.

The architecture identified for the instrument includes a central body that can house a connection element from which the displacement will then be measured. The connection element must connect the piston on one side and the displacement measuring device on the other. The connection element must also be correctly guided during its translation to avoid errors due to the inclination between the axes of the elements (i.e., between the central body and the connection element).

An instrument composed in this way can be equipped with any displacement measurement device. In fact, there are no dimensional constraints apart from those related to the presence of a rainwater collection tank, as the instrument can be housed in a dedicated head and placed in contact with the designed connection element. After considering the use of all displacement measurement systems, such as comparators, LVDTs, laser displacement sensors, and calipers, the design choice focused on the use of centesimal caliper technology. Other solutions were discarded because they were costlier and complex from a measurement chain perspective (LDTV, laser rangefinder) or did not meet the dimensional design constraints (laser displacement sensor, comparator). Conversely, the centesimal digital caliper is a very widespread, accurate, and economical measuring instrument. Furthermore, the electronics used for this type of device (ASIN B0BLS2BNHH Digital Caliper—Vinabo Max Intelligent Ltd., Hong Kong, China) are adaptable to the required measuring instrument. The centesimal resolution appears to be sufficient to evaluate the piston stroke variations following a deformation of the connecting rod caused by the overstresses described above. The choice will be validated by the results shown in Section 3 and is also compatible with the required specifications.

2.2. Design of the Instrument Components

Once the measurement sensor to use has been identified, the instrument's design is illustrated. As seen, the instrument consists of a central body, a threaded end, a connection element, guides, and a head that houses the displacement sensor. The components are described in detail in the following subsections.

2.2.1. Central Body and Threaded End

The central body is the part of the tool that fits inside the tubes made on the engine head to insert the ignition coil assembly. Another function of the body is to house the piston stroke connection element and ensure its correct positioning; therefore, it must be hollow. The central body must have a contact point with the engine head so that it rests securely on the reference surface chosen as the absolute reference point for the desired measurement. The cylinder head's thread reference surface, into which the spark plug is screwed, serves as a reference. The central body must therefore have a threaded end. However, it must be taken into account that the connection element must penetrate inside the cylinder that can reach the piston crown and follow its movement; therefore, the external threaded part at the end of the central body must also be hollow. However, obtaining a threaded end directly on the central body does not guarantee that the instrument will reach the reference surface due to the impossibility of completely threading the smaller cylindrical end thus created. This would therefore result in the tool finishing screwing not when the wider surface of the tool comes into contact with the head, but when the nut screw into which the tool is screwing meets the last complete thread on the external thread. This condition would not constitute a unique reference for the reference position of the measurement. It was therefore decided to create an externally threaded cylindrical element that is partially screwed into an internal thread made in the final part of the central body, and the remaining part will protrude from the central body. Once the components are screwed in, the central body can be attached to the engine cylinder head using the internal thread designed for the

spark plug, ensuring a secure contact, since, using a completely threaded protrusion, it will be possible to screw the instrument and have the contact surface of the instrument rest on that of the head.

The solution identified (Figure 2) allows the same central body to be used for engines with different spark plug threads by simply replacing the threaded insert (for example, M14 × 1.25). Thus, only the threaded end must be adapted to the various engines' interfaces.

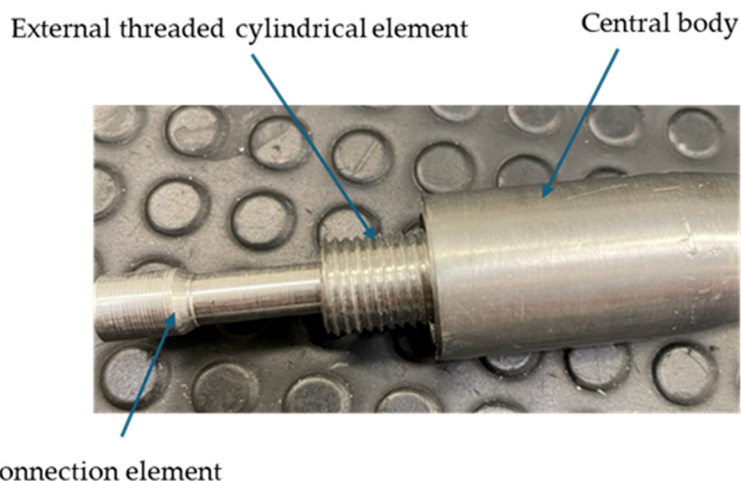


Figure 2. Threaded end of the tool.

Given the limited space above the engine head and the engine's position within the vehicle, the instrument must be inserted at an angle to fit into the cylinder head tubes without disassembling other parts. Therefore, it was decided to shape the central body by reducing its diameter in the central area to facilitate insertion. Regarding the radial dimension of the central body at the ends, on one side, it must ensure proper contact with the reference surface regardless of the thread size of the mounted threaded end, and on the other side, it must mate stably with the measuring instrument's interface.

The central body is sized to be longer than the tube of the head, which means that the upper end of this component can also have a larger diameter than the central area in order to accommodate the components that will be described later. The central body must also have a connection to the head of the instrument housing the measuring instrument (Figure 3). The two elements must be axially locked to avoid measurement errors.



Figure 3. Central body, threaded end, and connection element.

2.2.2. Connection Element and Guides

The purpose of the connection element, or probe, is to transmit the piston stroke to the inside of the instrument head; the probe's end will provide the displacement to be measured with the caliper. When the piston, approaching top dead center, contacts the probe, the latter is lifted; the probe's rise in turn causes the caliper rod to move, whose displacement is then read on the caliper's screen. It was decided to ensure contact between

the probe and the caliper rod exclusively by using the force of gravity, given the low rotation speeds of the crankshaft that will be used during measurements to move the pistons.

This connection element must be well-guided inside the central body in order to avoid measurement errors due to incorrect alignment; for this reason, the use of two guides made of low-friction material and consisting of sleeves composed, for reasons of ease of assembly, of two semi-circular crowns that wrapped around the central part of the connection element was envisaged.

2.2.3. Instrument Head

The head is the part of the instrument that houses the commercial measuring device. The instrument head and the central body must be axially locked to avoid any measurement errors during use of the instrument.

Furthermore, to allow measurement both with and without a dedicated interface, it was decided to maintain the ability to rotate the instrument head relative to the central body, allowing for a more adaptable viewing direction of the screen displaying the measurement. This way, an operator not using the dedicated interface can still screw the central body in place of the spark plug and then rotate the instrument head to the position most convenient for reading the displacement. To create this connection system, three grub screws positioned at 120° are screwed into the head and fit into a special groove in the central body (Figure 4). The groove is designed to accommodate the grub screws but prevents their axial movement.



Figure 4. Instrument head with caliper screen.

It is also planned to insert the upper end of the central body into the head, inside which a stop will be made in order to bring the central body into a certain position.

The head is designed to completely accommodate the gauge shield, protecting it from any impact and damage during use. Likewise, to prevent possible damage to the gauge's graduated rod, the length of the head is sized so that when the piston is at top dead center and therefore in the highest position of the return element and consequently of the rod, the rod does not protrude from the head but remains protected inside.

2.3. Instrument Calibration

The instrument as designed can be used on any spark ignition engine; however, due to the different sizes of dead volumes and the different shapes of piston heads, the instrument must first be calibrated for each type of engine. Furthermore, the instrument provides indications of the piston stroke by referring to the spark plug contact surface; however, this indication is not useful for practical application in workshops. It is therefore necessary for a calibration phase to be carried out prior to the measurement phase using a special accessory. It will therefore proceed to implement, for each type of motor, a special threaded parallelepiped with a hole of a depth exactly equal to the measurement of the piston

crown position of the engine being tested when it is at top dead center. These calibration accessories will be supplied with the instrument and used in the measurement procedure. In order to produce the appropriate accessories, for each type of engine, the piston stroke is measured with the instrument following the measurement procedure (which is described in Section 2.4) on a reference engine, for example, a new engine. Once the minimum measurement value has been reached, the instrument is reset to zero using the appropriate button on the head of the instrument. Once the zero point has been defined, the accessory described can be manufactured.

2.4. Instrument Accuracy

Once the instrument was completed and calibrated for one type of engine, its accuracy was tested. To this end, the instrument was installed and removed several times, performing a large number of measurements (approximately one hundred) to see if the instrument provided the same measurement. For all measurements taken, a difference of just 1 hundredth of a millimeter was noted in the values provided. It was not possible to establish the precision of the instrument as there are no similar instruments with which to compare the measured values.

2.5. Instruments User Interface

To comply with the project specifications, a hardware and software interface was designed and built that the operator could interact with to perform the tests. This interface is essential for carrying out measurements with a single operator and must therefore allow a busy mechanic moving the crankshaft to read the piston stroke measurement. The interface must also facilitate the storage of the acquired data.

2.5.1. Interface Specifications

The interface to be developed must meet the following specifications: have good visibility and be positioned wherever is most convenient for the operator; display the values of the measurements taken by the instrument in a legible format; allow for interaction with the operator to enter the vehicle's references being measured; and record the vehicle's references, date, time, and measurements taken on a memory device. To protect the system, a box has been created to house these components. The only limitation of the interface's size is its ease of handling and the readability of the information provided by the operator.

2.5.2. Signal Output and Communication Protocol

The caliper's integrated electronic can provide the measurement obtained through two digital outputs: the clock line and the data line. It is important to identify the protocol the caliper uses to communicate the data. For this purpose, the output is detected using an oscilloscope. Connect the caliper board's ground to the oscilloscope, the data line to channel 1, and the clock line, which is responsible for determining the information sampling time, to channel 2.

It is possible to note that each measurement is composed of six packets of four bits each; the first five packets refer to the numerical information of the measurement expressed in binary form, while the last packet contains information on the sign, the unit of measurement, and the presence of a decimal point in the case of measurements in inches.

The caliper is powered by a 1.5 V battery, so the outputs are characterized by a high voltage value of approximately 1.4 V; to interpret the signal as digital, the voltage value of the high signal must be 5 V. A circuit was therefore designed to raise the value to 5 V through the use of an operational amplifier whose objective is to compare two voltage levels. Therefore, by setting a reference voltage value on the inverting input, if a higher voltage level arrives at the non-inverting input, the output will be the comparator's power

supply value (in this case set to 5 V); conversely, if the voltage level of the non-inverting input is lower than the reference value, the output will be zero.

A circuit was created (Figure 5) using an LM393P integrated circuit (Texas Instruments, Dallas, TX, USA), chosen because it directly integrates two comparators, one of which is used to raise the voltage level of the data line and the other for the clock line. To test feasibility, the resulting 5 V digital output of the gauge was processed with an Arduino-UNO R3 controller (Arduino Srl, Torino, Italy) connected to a two-line, sixteen-character liquid crystal display. Code has been compiled to duplicate the information on the caliper on the liquid crystal display.

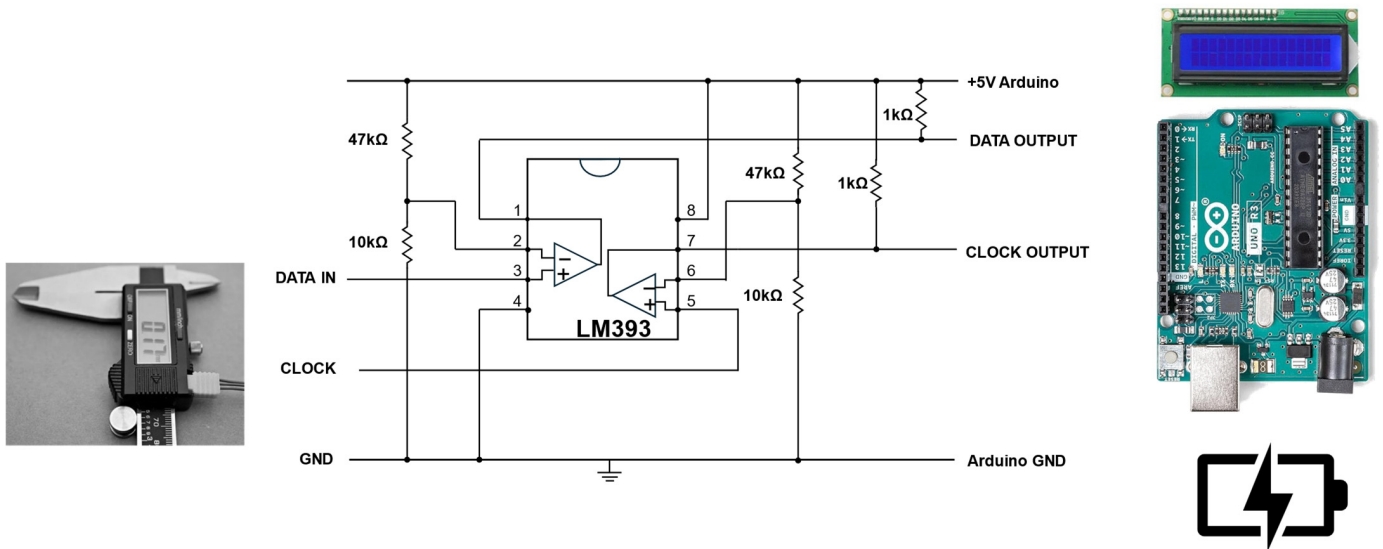


Figure 5. Duplication of measurement information on Arduino-managed screen: circuit diagram and connections scheme.

2.5.3. HW/SW Interface Design

Based on the specifications above, the following hardware components required for the project were identified: a microcontroller with sufficient inputs and outputs to connect and manage all the components, a touch screen of appropriate size, the specially designed electronic circuit (see Section 2.5.2) for transforming the signals into digital output, an Arduino-compatible shield for a Micro SD memory card, an Arduino-compatible shield for the date and time, an appropriate connector for connection to the instrument, push buttons, a terminal block to facilitate connections between the components and the controller, and finally a system that guaranteed power to the system for a large number of uses.

The controller used was an Elegoo Mega 2560 R3 (Elegoo, Inc., Shenzhen, China); the choice stemmed from the number of available inputs and outputs compatible with the project’s needs. For a good compromise between practicality and readability, a 3.5-inch touch screen was chosen. The shields for the clock (RTC AT42C32 IIC—Shenzhen Ruizhi Electronics Ltd., Shenzhen, China) and the memory card (Micro SD TF 6Pin SPI—HiLetgo Technology Co., Ltd., Shenzhen, China) were also identified. To allow the instrument to be screwed and unscrewed from the spark plug socket, the interface must be connected to it only after this operation. For this purpose, a USB Type A interface can be used, allowing the instrument to be released from the interface for insertion and removal operations from the measuring position.

The interface features four 2-pin normally open push buttons with different colored caps to perform the various functions. The terminal block was chosen based on the controller used, opting for the Mega 2560 R3 Terminal Block Breakout Board HAT. For power, a commercial power bank with a 5000 mAh rechargeable lithium battery was

used. This capacity is adequate because it allows for several hundred measurements to be performed before needing to be recharged.

Figure 6 shows a scheme of the interface and instrument connections.

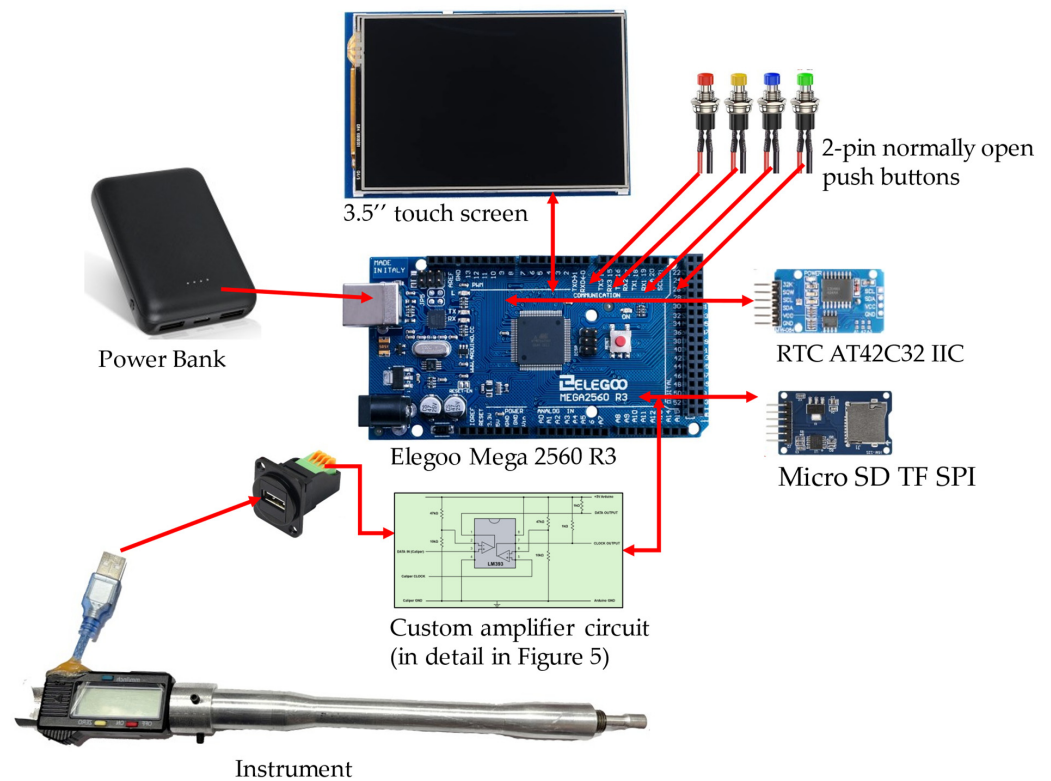


Figure 6. Scheme of the interface and instrument connections.

Once the hardware components are assembled, a code is compiled for the controller to execute. This code performs all the necessary operations to correctly collect the analysis input information and subsequently the measurement procedure, as described in Section 2. The system is designed to be operated with both physical push buttons and a touchscreen, ensuring greater versatility. The system generates both usable information directly on-screen and a file that is saved to the memory card. Figure 7 shows the screen displayed during the measurement operations.



Figure 7. The measurement screen contains information relating to the piston being measured: (A), the current piston stroke (B), the minimum stroke recorded so far (C), and the minimum stroke values recorded for previously measured pistons (D). Touch buttons for performing specific operations during the measurement (E).

2.6. Definition of the Measurement Procedure

The measurement procedure to be used is illustrated in the diagram in Figure 8.

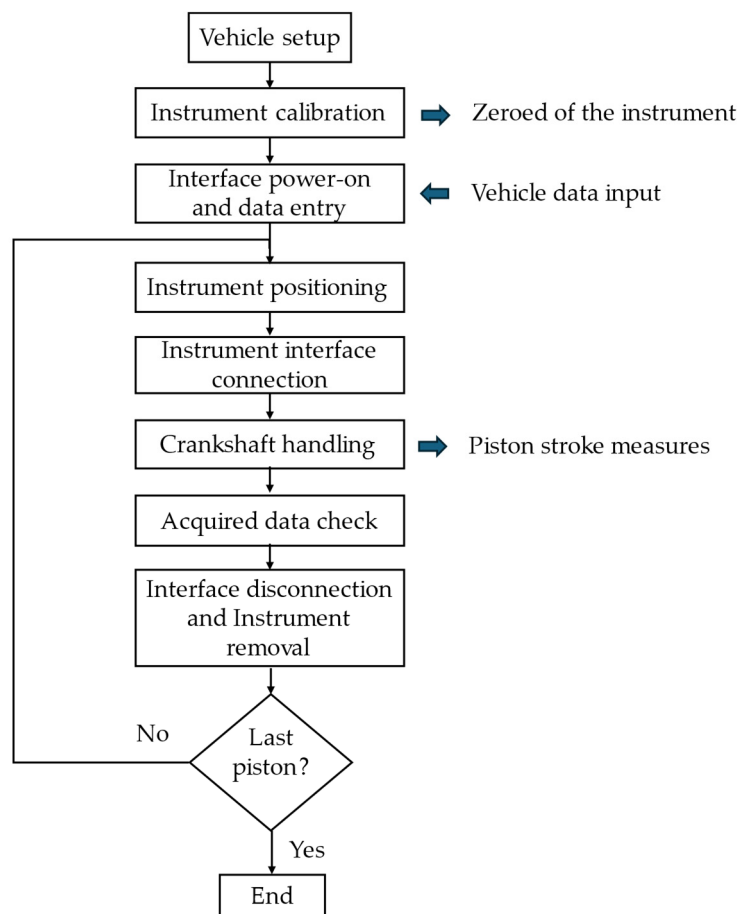


Figure 8. Measurement procedure.

The first step of the procedure is the preparation of the vehicle for the measurement operations, i.e., disconnecting the ignition coil assembly connectors, removing the bolt and the ignition coil assembly from the cylinder hand-cover, and unscrewing the spark plug. This operation must be performed on all cylinders. In this case, the design specifications were also followed, as the operations to be performed on the engine are minimally invasive and require minimal, non-specialized labor.

The instrument is then calibrated. This operation is performed by screwing the instrument into the special accessory specific for the analyzed engine (as described in Section 2.3). Once the instrument is screwed in fully, the measurement is zeroed using the special button on the instrument head. Once unscrewed from the accessory, the instrument is calibrated and ready for measurement. At this point, turn on the interface and enter all the required vehicle data: vehicle identification number, mileage, and engine type. Next, screw the tool in place of the spark plug on the first piston. Connect the instrument to the interface (Figure 9).

The crankshaft is moved manually by checking through the interface that at least three complete revolutions have been made. Check the data acquisition and press the button that allows you to move on to the next piston stroke measurement. Disconnect the tool from the interface and remove it from the spark plug seat. Repeat the insertion and subsequent steps for all remaining pistons. After measuring the last piston, press the button to advance to the next measurement. The program will display a message indicating that all pistons

have been measured and will close the file containing all of the vehicle references entered, the date and time, and all acquired measurements.



Figure 9. System positioned for measurement.

3. Results and Discussion

As required by the specifications, checking the deformation of the connecting rods performed using the proposed instrument is easy and economical; in fact, the duration of the verification procedure was evaluated during the experimental validation, and it was always found to be less than 20 min for three-cylinder engines. The overall costs of the system were maintained under 120 €, assuring the possibility of easy diffusion in car repair shops.

To validate the capability of the instrument, an experimental campaign was implemented. The data collected relates to 20 cars with the same engine model (engine specifications details are listed in Table 1) and with mileage between 0 and 90,000 km.

Table 1. Summary of the data of the engines used for the experimental campaign: Miller cycle engine 1.5 cc for hybrid application.

Element	Specific	Unit
No. of Cyls. & Arrangement	3-cylinder, In-line	
Displacement	1490	cm ³
Bore × Stroke	80.5 × 97.6	mm
Compression Ratio	14.0:1	
Max. Output (EEC)	68@5500	kW@rpm
Max. Torque (EEC)	120@3600 to 4800	N × m@rpm
Valve Timing Intake Open	−30° to 40° BTDC	
Valve Timing Intake Closed	110° to 40° ABDC	
Valve Timing Exhaust Open	3° to 44° BBDC	
Valve Timing Exhaust Closed	41° to 0° ATDC	
Firing Order	1–2–3	

Three measurements were taken for each cylinder according to the procedure outlined in Section 2.6. This approach allowed for an assessment of the variability in piston stroke

resulting from various factors, including those associated with production. Specifically, the analysis focused on variability due to differences between cylinders, variability arising from differences among the tested engines, and variability linked to component wear, which can be evaluated in relation to mileage. To investigate the impact of mileage, the database was categorized into two groups: those with mileage under 60,000 km and those exceeding 60,000 km.

The results were analyzed statistically, indicating that the effect of the cylinder was not statistically significant (p -value > 0.5). In contrast, the effect of mileage was statistically significant, although it was negligible in relation to the overall variability measured (adjusted R-squared approximately 10%). It was determined that mileage impacted piston stroke by no more than 0.012 mm (95% CI: 0.02–0.12 mm).

Figure 10 shows the overall variability of the data. The natural variability of this measurement (mean ± 3 standard deviations) is between 0.221 mm and -0.241 mm. Considering that the effect of incorrect refueling on permanent deformation of the connection rod and consequently on piston stroke variation was found to be greater than 0.6 mm (as confirmed in [27]), it can be seen that the Z-score is equal to 7.9. This indicates that the developed measurement system can correctly detect this type of damage, regardless of the overall variability of the measurement due to the effects of the other analyzed factors.

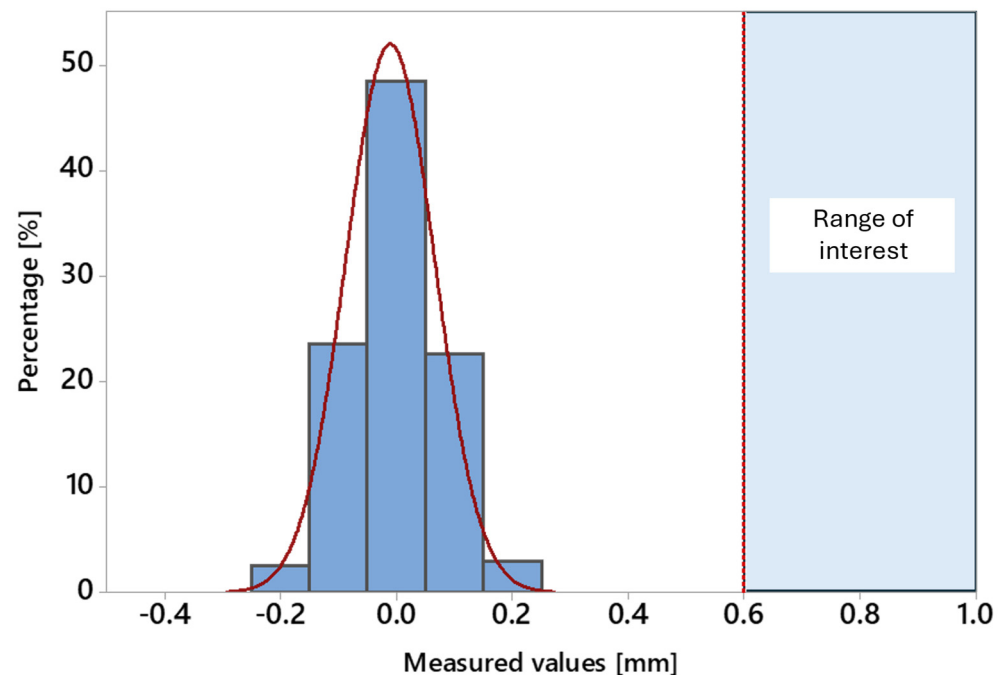


Figure 10. Results of the experimental campaign in terms of piston stroke variation (mean = -0.01 mm, Standard Deviation = 0.077 mm) and the range of interest for piston stroke variation due to incorrect refueling (greater than 0.6 mm [27]).

4. Conclusions

The study's results indicate that the measuring instrument developed is able to detect the deformation of the connection rod related to incorrect fueling in hybrid cars powered with gasoline.

In particular, the prototype tested showed a high level of Z-score with regard to its ability to differentiate between the usual technological variability of the piston stroke and the range that can be connected to the anomaly studied.

From the point of view of the duration of the measurement procedure, the approach appears very interesting and is able to permit the procedure in less than 20 min for a whole

engine instead of about 20 h in the current procedure. Finally, it can be observed that the developed instrument is composed of basic mechanical elements and uses commercially available electronic components that are easily replaceable.

In future works, it will be interesting to characterize the damage of a broken connecting rod with direct measurement on failed engines and to extend the measurement campaign to a larger population of cars as well as a higher mileage.

Author Contributions: Conceptualization, V.L.B., L.D.P., S.M., A.G. and G.A.; methodology, V.L.B., L.D.P., S.M. and A.G.; software, V.L.B., L.D.P. and A.G.; validation, S.M.; formal analysis, V.L.B. and A.G.; investigation, V.L.B., L.D.P., S.M. and A.G.; data curation, V.L.B., L.D.P. and A.G.; writing—original draft preparation, V.L.B., S.M. and A.G.; writing—review and editing, V.L.B., L.D.P., S.M., A.G. and G.A.; visualization, V.L.B. and A.G.; supervision, G.A. All authors have read and agreed to the published version of the manuscript.

Funding: This research received no external funding.

Data Availability Statement: Dataset available on request from the authors.

Conflicts of Interest: The authors declare no conflicts of interest.

References and Note

1. Saeed, M.A.M.; Aly, M.M.; Abu-Elwfa, S. A Review on Hybrid Electrical Vehicles: Architectures, Classification and Energy Management. *SVU-Int. J. Eng. Sci. Appl.* **2024**, *5*, 93–99. [[CrossRef](#)]
2. Zhang, F.; Wang, L.; Coskun, S.; Pang, H.; Cui, Y.; Xi, J. Energy Management Strategies for Hybrid Electric Vehicles: Review, Classification, Comparison, and Outlook. *Energies* **2020**, *13*, 3352. [[CrossRef](#)]
3. Aliberti, D.; Ortenzi, F.; La Battaglia, V.; Marini, S.; Vellucci, F. Evaluation of the Efficiency of a Hybrid ICE Vehicle Fuelled with Hydrogen Compared with a Fuel Cell Vehicle, Based on a Simulation Model. *J. Phys. Conf. Ser.* **2023**, *2648*, 012082. [[CrossRef](#)]
4. Sun, X.; Dong, Z.; Cai, Y.; Jin, Z.; Lei, G.; Tian, X. A Comprehensive Review of Design Optimization Methods for Hybrid Electric Vehicles. *Renew. Sustain. Energy Rev.* **2025**, *217*, 115765. [[CrossRef](#)]
5. Giorgetti, A.; Rolli, F.; La Battaglia, V.; Marini, S.; Arcidiacono, G. Axiomatic Design Using Multi-Criteria Decision Making for Material Selection in Mechanical Design: Application in Different Scenarios. In *Proceedings of the 15th International Conference on Axiomatic Design 2023, ICAD 2023*; Puik, E., Cochran, D.S., Foley, J.T., Foith-Förster, P., Eds.; Lecture Notes in Networks and Systems; Springer Nature: Cham, Switzerland, 2023; pp. 135–148. [[CrossRef](#)]
6. Vicente, A.T.D.; Camperos, M.C.; Almonacid-Durán, M. The Evolution of Electric and Hybrid Vehicles and Their Influence on Sustainable Transport: A Review and Future Research Lines. *Sustain. Technol. Entrep.* **2025**, *4*, 100100. [[CrossRef](#)]
7. Ferrara, D.; Cicconi, P.; Minotti, A.; Trovato, M.; Caputo, A.C. New Space Engineering Design: Characterization of Key Drivers. *Appl. Sci.* **2025**, *15*, 8138. [[CrossRef](#)]
8. Amicarelli, M.; Trovato, M.; Cicconi, P. Lightweight Design of a Connecting Rod Using Lattice-Structure Parameter Optimisation: A Test Case for L-PBF. *Machines* **2025**, *13*, 171. [[CrossRef](#)]
9. Milojević, S.; Savić, S.; Marić, D.; Stopka, O.; Krstić, B.; Stojanović, B. Correlation between Emission and Combustion Characteristics with the Compression Ratio and Fuel Injection Timing in Tribologically Optimized Diesel Engine. *Teh. Vjesn.—Tech. Gaz.* **2022**, *29*, 1210–1219. [[CrossRef](#)]
10. Żółtowski, B.; Wojciechowski, H.; Castaneda, L. Selected Problems of Maintaining the Serviceability of Turbochargers. *MATEC Web Conf.* **2023**, *375*, 01006. [[CrossRef](#)]
11. Xu, X.; Wang, H.; Zhang, N.; Liu, Z.; Wang, X. Review of the Fault Mechanism and Diagnostic Techniques for the Range Extender Hybrid Electric Vehicle. *IEEE Access* **2017**, *5*, 14234–14244. [[CrossRef](#)]
12. Shoultz, L.W. Implementation of Design Failure Modes and Effects Analysis for Hybrid Vehicle Systems. Doctoral Dissertation, Virginia Tech, Blacksburg, VA, USA, 2016.
13. Blaabjerg, F.; Wang, H.; Vernica, I.; Liu, B.; Davari, P. Reliability of Power Electronic Systems for EV/HEV Applications. *Proc. IEEE* **2020**, *109*, 1060–1076. [[CrossRef](#)]
14. Tang, Q.; Shu, X.; Zhu, G.; Wang, J.; Yang, H. Reliability Study of BEV Powertrain System and Its Components—A Case Study. *Processes* **2021**, *9*, 762. [[CrossRef](#)]
15. La Battaglia, V.; Mussi, V.; Marini, S.; Giorgetti, A. Investigation of Damage Caused by Chlorine-Contaminated Fuel in Standard Vehicle Components. *Eng. Proc.* **2025**, *85*, 8. [[CrossRef](#)]
16. Jiang, X.; Hu, J.; Peng, H.; Chen, Z. A Design Methodology for Hybrid Electric Vehicle Powertrain Configurations with Planetary Gear Sets. *J. Mech. Des.* **2020**, *143*, 083402. [[CrossRef](#)]

17. Mohammadpour, M.; Theodossiades, S.; Rahnejat, H. Dynamics and Efficiency of Planetary Gear Sets for Hybrid Powertrains. *Proc. Inst. Mech. Eng. Part C J. Mech. Eng. Sci.* **2015**, *230*, 1359–1368. [[CrossRef](#)]
18. Doppelbauer, M. Hybrid Vehicle Drives. In *Introduction to Electromobility*; Springer: Wiesbaden, Germany, 2024; pp. 41–77.
19. León, R.; Montaleza, C.; Maldonado, J.L.; Tostado-Véliz, M.; Jurado, F. Hybrid Electric Vehicles: A Review of Existing Configurations and Thermodynamic Cycles. *Thermo* **2021**, *1*, 134–150. [[CrossRef](#)]
20. Perceau, M.; Guibert, P.; Guilain, S.; Segretain, F.; Redlinger, T. Why Can Miller Cycle Improve the Overall Efficiency of Gasoline Engines? In Proceedings of the THIESEL 2020 Conference on Thermo- and Fluid Dynamic Processes in Direct Injection Engines, Valencia, Spain, 8–11 September 2020.
21. Holjevac, N.; Cheli, F.; Gobbi, M. Multi-Objective Vehicle Optimization: Comparison of Combustion Engine, Hybrid and Electric Powertrains. *Proc. Inst. Mech. Eng. Part D J. Automob. Eng.* **2019**, *234*, 469–487. [[CrossRef](#)]
22. Brooker, A.D.; Ward, J.; Wang, L. Lightweighting Impacts on Fuel Economy, Cost, and Component Losses. *SAE Tech. Pap. CD-ROM/SAE Tech. Pap. Ser.* **2013**, *1*, 10. [[CrossRef](#)]
23. Solomon, A.; Battiston, P.; Sczomak, D. Lean-Stratified Combustion System with Miller Cycle for Downsized Boosted Application—Part I. *SAE Int. J. Adv. Curr. Pract. Mobil.* **2021**, *3*, 1666–1681. [[CrossRef](#)]
24. Battiston, P.; Wheeler, J.; Solomon, A.; Sczomak, D. Lean-Stratified Combustion System with Miller Cycle for Downsized Boosted Application—Part 2. *SAE Int. J. Adv. Curr. Pract. Mobil.* **2021**, *3*, 1651–1665. [[CrossRef](#)]
25. Brusa, A.; Corti, E.; Rossi, A.; Moro, D. Enhancement of Heavy-Duty Engines Performance and Reliability Using Cylinder Pressure Information. *Energies* **2023**, *16*, 1193. [[CrossRef](#)]
26. Zeilinga, S.; Rottengruber, H.; Dafis, A.; Wagner, A.; Stolt, T.; Feikus, F.J. Investigation of Deviations in SI-Engine Behaviour Due to Manufacturing Tolerances in Cylinder Heads. *Automot. Engine Technol.* **2021**, *6*, 147–158. [[CrossRef](#)]
27. Fini, S. Technical report, Relazione di Consulenza Tecnica di Ufficio, Tribunale di Milano—Quarta Sezione Civile r.g.9638/2025. 2025.

Disclaimer/Publisher’s Note: The statements, opinions and data contained in all publications are solely those of the individual author(s) and contributor(s) and not of MDPI and/or the editor(s). MDPI and/or the editor(s) disclaim responsibility for any injury to people or property resulting from any ideas, methods, instructions or products referred to in the content.